catalysts

MDPI

Article

Palm Biochar-Based Sulphated Zirconium (Zr-AC-HSO_3) Catalyst for Methyl Ester Production from Palm Fatty Acid Distillate

Umer Rashid [1,*], Soroush Soltani [2], Thomas Shean Yaw Choong [2], Imededdine Arbi Nehdi [3,4], Junaid Ahmad [5] and Chawalit Ngamcharussrivichai [6]

1 Institute of Advanced Technology, Universiti Putra Malaysia, Serdang 43400, Selangor, Malaysia
2 Department of Chemical and Environmental Engineering, Engineering Faculty, Universiti Putra Malaysia, Serdang 43400, Selangor, Malaysia; soroush.soltaani@gmail.com (S.S.); csthomas@upm.edu.my (T.S.Y.C.)
3 Chemistry Department, College of Science, King Saud University, Riyadh 11451, Saudi Arabia; inahdi@ksu.edu.sa
4 UR Physico-Chimie des Matériaux Solides, Chemistry Department, Science College, Tunis El Manar University, Tunis 2092, Tunisia
5 Department of Chemical Engineering, Khalifa University, Abu Dhabi 127788, UAE; Junaid.faridi@ku.ac.ae
6 Center of Excellence in Catalysis for Bioenergy and Renewable Chemicals (CBRC), Faculty of Science, Chulalongkorn University, Bangkok 10330, Thailand; Chawalit.Ng@chula.ac.th
* Correspondence: umer.rashid@upm.edu.my; Tel.: +60-3-97697393

Received: 11 October 2019; Accepted: 28 October 2019; Published: 5 December 2019

Abstract: A palm waste kernel shell biomass was converted into bio-based sulphonated activated carbon and further used for preparation of a sulphated zirconium-doped activated catalyst (Zr-AC-HSO_3) by wet impregnation method. The structural, physicochemical, morphological, textural, and thermal characteristics of the synthesized Zr-AC-HSO_3 catalyst were characterized by X-ray diffraction (XRD), Brunauer–Emmett–Teller (BET) surface area analysis, temperature-programmed desorption of ammonia (TPD-NH_3), Fourier transform infrared spectroscopy (FT-IR), and scanning electron microscopy (SEM). The catalytic activity of the 20 wt% Zr-AC-HSO_3 catalyst was further evaluated for esterification of palm fatty acid distillate (PFAD). This study achieved a maximum fatty acid methyl ester (FAME) yield of 94.3% and free fatty acid (FFA) conversion of 96.1% via the esterification over 20 wt% Zr-AC-HSO_3 using 3 wt% catalyst concentration, 15:1 methanol:PFAD molar ratio at 75 °C for 3 h. The experiments to test for reusability showed that the spent catalyst was stable for five successive reaction cycles, with a FFA conversion of 80% in the fifth cycle, without additional treatment. The critical fuel features of the synthesized PFAD methyl ester were determined and were within the range of EN14214 and ASTM D6751 standards.

Keywords: Sulfonated palm-based catalyst; wet impregnation method; palm fatty acid distillate (PFAD); esterification; fatty acid methyl ester production

1. Introduction

Energy demands are continually increasing, globally, due to increases in population and technology [1,2]. The energy needed to produce goods and other services, such as transportation, is still mainly provided by conventional fossil fuels. Apart from the possible future depletion of the oil reserves, fossil fuels are associated with some major environmental issues. Global warming, environmental pollution, poisonous exhaust from internal combustion engines, and their non-biodegradable nature are severe concerns and long-term threats for humans and aquatic life [3,4]. These reasons have encouraged the search for renewable resources, as alternatives to conventional fossil fuels.

Biodiesel is considered as a trustworthy alternative energy source to conventional fuels because of the easy availability of the feedstock, similar combustion properties, lower toxicity and biodegradable nature, which makes it more environmentally friendly [5–7]. Conventionally, biodiesel is produced on a commercial scale through the processes of free fatty acid (FFA) esterification and vegetable oil transesterification over heterogeneous or homogeneous catalysts in the presence of an appropriate alcohol. However, whilst homogeneous catalysts can speed up the reaction at low temperatures (<65 °C), their separation from esters is very difficult and it requires large amounts of water for the purification process [8]. Besides that, the homogeneous catalysts are mostly used for feedstocks that contain less FFA content (<1%) or for virgin oil. This content can be mostly found in edible types of feedstock, which are expensive and, consequently, make biodiesel production expensive and create the fuel versus food controversy. Because of these drawbacks, the focus of research studies has now been put onto catalysts that are heterogeneous.

Heterogeneous solid base catalysts are regarded as sustainable catalytic systems that possess more unique characteristics as compared to homogeneous catalyst systems, such as easy separation, easy disposal, and being generally less toxic [9]. Base catalysts that are solid are very popular during the process for transesterifying triglycerides (TGs) into fatty acid methyl ester (FAME). However, solid base catalysts are only able to transesterify feedstock with less than 3% FFA in a single-step process, otherwise pretreatment of feedstock is required to lower the FFA <1% for transesterification into FAME to take place [10]. However, solid acid catalysts that are heterogeneous potentially convert the feedstock containing >90% FFA to FAME. Therefore, in the case of feedstocks with higher acid values, using a heterogeneous acid catalyst provides a much better performance than using a solid base catalyst.

Choosing the right feedstock plays a prominent part in improving the conversion rate with a lower cost. More than 70% of the biodiesel fuel production cost comes from the feedstock, which is why biodiesel is so expensive compared to conventional fossil fuel [11]. Amongst all the known crude oils, palm oil has drawn the most recent attention. Malaysia is known as the second largest producer and exporter of palm oil in the world. There has been an increase in the production of palm oil in Malaysia over the past few years. In 2017, production was recorded at 19.9 million tones, which was an increase from 1985, which was recorded at 4.1 million tones. Resulting from the massive amount of palm oil is an increasing amount of palm oil waste material, starting from palm tree trunks and leaves to palm kennel shells. However, recently in the advent of bio-fuels, the palm oil waste materials are no longer considered as waste as they are now being utilized for catalysts and biodiesel production [12]. Palm fatty acid distillate (PFAD) is a by-product obtained from the refinery process of the crude palm oil. It has a large amount of FFA (around 90%) and is inexpensive. Utilization of the PFAD as a feedstock to generate ester would help in the commercialization of the process as a result of its availability and low cost [13,14].

Biomass materials, such as palm kernel shells, have been utilized as carbon precursors to synthesize solid acid catalysts that are carbon based. This is achieved through the process of carbonization under a nitrogen flow [15]. Carbon-based solid acid catalysts possess a large surface area, a stable framework, and are water-tolerant. Because of these properties, they are believed to give high catalytic activity against feedstocks that contain very high FFA [16]. Most of the carbon materials are inexpensive and usually obtained from waste materials. In addition, they can be easily modified with other transition metal oxides and the sulphonic group (–SO_3H) through the impregnation and post-sulphonation processes, respectively [17]. So far, novel heterogeneous catalysts, which are carbon-based solid acids, have been synthesized using various types of biomass. Sulphonated activated carbon-based biochar [18], sulphonated carbohydrate-derived solid acid catalysts [19], and sulphonated sugarcane bagasse [20] are the most commonly synthesized catalysts of carbon-based solid acids used for generation of biodiesel. In 2015, a sulphonated glucose acid catalyst (SGAC) was used to carry out the PFAD esterification [21]. The FFA conversion 94.5% was obtained under the optimum conditions,

a 12.2:1 methanol:PFAD molar ratio, 2.9% catalyst loading, 65 °C reaction temperature and 134 min reaction time.

This research aimed to evaluate the detailed characterization of a synthesized zirconium oxide (ZrO_2)-doped sulphonated biochar catalyst and its catalytic activity for esterification of PFAD. In the present work, the wet impregnation technique was introduced to fabricate the biochar-based sulphated zirconium-doped activated carbon heterogeneous solid acid (Zr-AC-HSO_3) catalyst. Meanwhile, the textural, structural, thermal, morphological, and physicochemical characteristics of the synthesized catalyst were studied in detailed. Furthermore, the synthesized catalyst was analyzed to determine its functionality to produce FAME. The impacts of the operational conditions, which were the methanol:PFAD molar ratio, reaction temperature, time, and catalyst loading for the esterification reaction were also studied. Moreover, the fuel properties of the synthesized ester were evaluated, as well as deliberated on in light of the European (EN 14214) and American Society for Testing and Materials (ASTM D6751) standards.

2. Results and Discussion

2.1. Correlation between the NH_3 Absorption and the FFA Conversion Rate

The catalytic activity of the fabricated Zr-AC-HSO_3 catalyst in the esterification of PFAD was determined under the initial reaction conditions using a methanol:oil ratio of 15:1 and catalyst amount of 5 wt% at 75 °C for 4 h The results is shown in Figure 1. Five different loadings of ZrO_2 (5, 10, 15, 20, and 25 wt%) were added over the sulphonated activated carbon (AC-HSO_3). It was observed that by increasing ZrO_2 concentrations from 5 wt% to 25 wt%, the acid density increased. However, the highest FFA conversion 85.4% was achieved over the 20 wt% Zr-AC-HSO_3 catalyst. According to the obtained results, 20 wt% Zr-AC-HSO_3 was used for further experimentations.

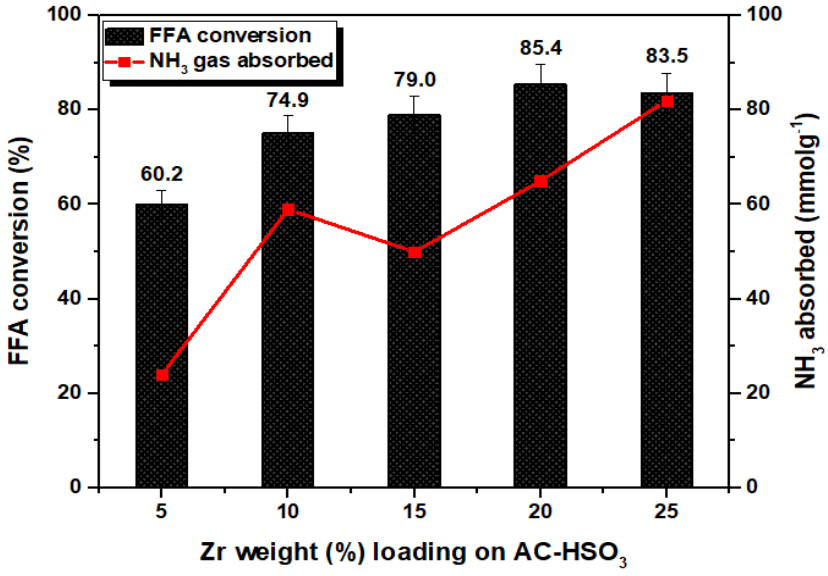

Figure 1. Correlation between the amount of NH_3 adsorbed and FFA conversion.

2.2. Catalyst Characterization

2.2.1. TPD-NH_3 Analysis

The method known as the temperature programmed desorption of ammonia (TPD-NH_3) was applied to evaluate the level of acidity of the synthesized 20 wt% Zr-AC-HSO_3 catalyst. The desorption peaks appeared on the TPD-NH_3 profile at various temperature zones, showing the strength of the heterogeneous solid catalyst. Two desorption curves were observed on the plot of TPD-NH_3 data in the

ranges of 155–280 °C and 500–610 °C, which were attributed to the existence of weak Bronsted/Lewis acid sites and strong Bronsted/Lewis acid sites, respectively [22,23], as seen in Figure 2a.

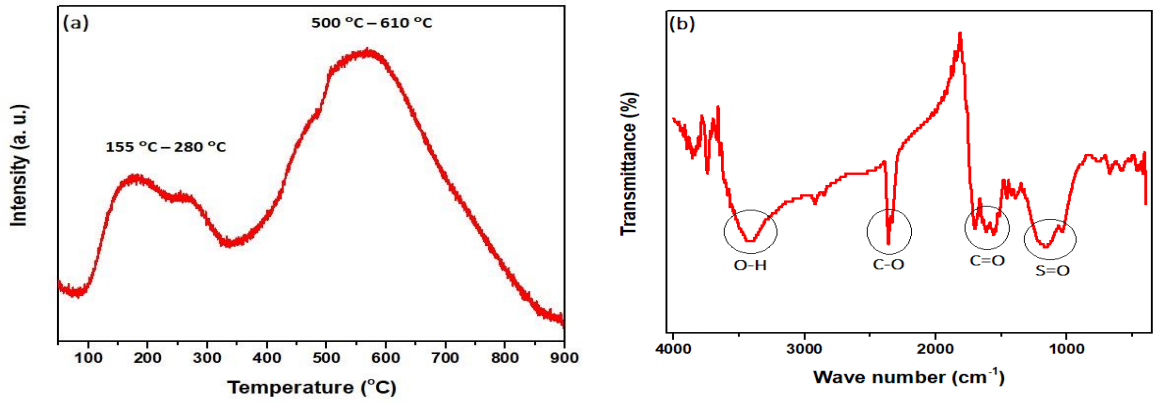

Figure 2. (**a**) TPD-NH_3 profile and (**b**) FT-IR spectrum of the synthesized 20 wt% Zr-AC-HSO_3.

2.2.2. FT-IR Analysis

The FT-IR vibration bands were used to confirm the functional groups attached to the surface of the synthesized catalyst as depicted in Figure 2b. The vibration band appearing at 3430 cm^{-1} confirmed the existence of O–H stretching mode on surface of Zr-AC-HSO_3 catalyst. The vibration bands at 2365 cm^{-1} and 1554–1698 cm^{-1} corresponded to the existence of C–O and C=O groups on the Zr-AC-HSO_3 surface, respectively. The stretching mode at 1152 cm^{-1} corresponded with the presence of –SO_3H group as an active site. It revealed that the sulphonic acid groups were successfully attached to the surface of the synthesized catalyst [24].

2.2.3. BET Surface Area Analysis

The N_2 adsorption–desorption isotherm and pore size distribution of the synthesized 20 wt% Zr-AC-HSO_3 catalyst are displayed in Figure 3a,b, respectively. The shape of isotherm was type IV with a type H3 hysteresis loop, as per the Brunauer, Deming, Deming, and Teller (BDDT) isotherm categorization. In the initial phase of the isotherm (P/Po < 0.4), adsorption of N_2 was weak, while in the middle phase (P/Po > 0.4), the increased adsorption, indicated the presence of monomodal mesopore size distribution. The sharp curve at 3.55 nm showed the pore diameter was monomodal, as shown in Figure 3b. The obtained textural characteristics of the synthesized 20 wt% Zr-AC-HSO_3 catalyst are summarized in Table 1.

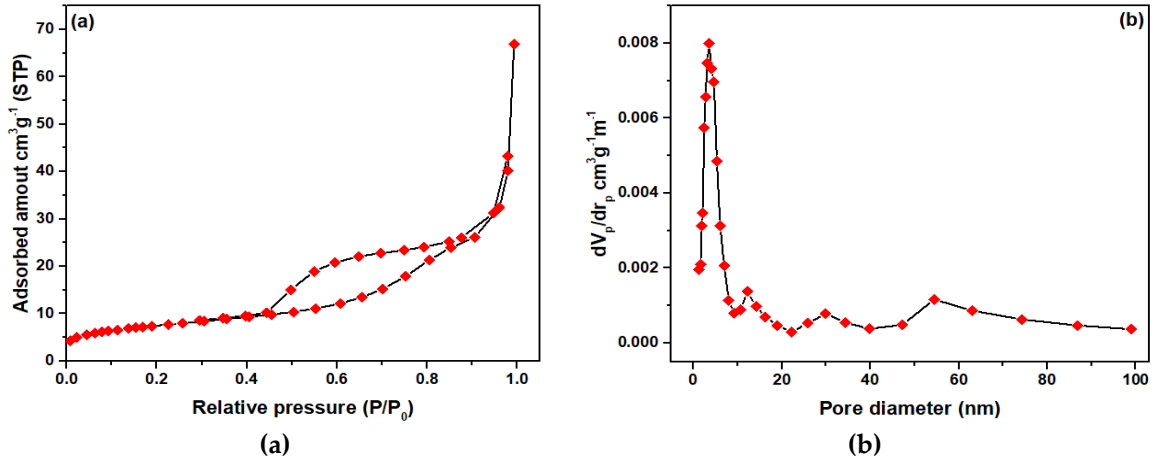

Figure 3. (**a**) N_2 adsorption-desorption isotherm and (**b**) BJH pore size distributions of the synthesized 20 wt% Zr-AC-HSO_3 catalyst.

Table 1. Textural characteristics of the synthesized 20 wt% Zr-AC-HSO_3 catalyst.

Sample	S_{BET} (m^2g^{-1}) [a]	D_p (nm) [b]	V_p (cm^3g^{-1}) [c]	NH_3 Acidity Density (mmol g^{-1}) [d]
20 wt%Zr-AC-HSO_3	326.71	3.55	0.32	19.55

[a] Specific surface area; [b] Average pore size; [c] Total pore volume at P/P_o = 0.99; [d] Based on NH_3-TPD measurements.

2.2.4. X-ray Diffraction Analysis

The XRD patterns of synthesized AC-HSO_3 and 20 wt% of Zr/AC-HSO3 catalysts are illustrated in Figure 4. The XRD spectrum of AC-HSO_3 represents an amorphous carbon structure. The broad carbon C (002) diffraction peak in the range of 15–30° confirmed the amorphous carbon structure. There was another weak C (101) diffraction peak in the range of 40–50°, which represents the graphite structure [25]. On the other hand, the Zr-AC-HSO_3 catalyst revealed the reflection peaks at 30.11°, 35.52°, 50.41°, 59.52°, and 62.46°, respectively corresponding to (111), (200), (220), (302), and (311) planes of monoclinic zirconia (JCPDS Card No.79–1771) [26]. From the XRD result, ZrO_2 was present only in the monoclinic phase and not the tetragonal or cubic phase. The single-phase presence of ZrO_2 confirms a high level of purity.

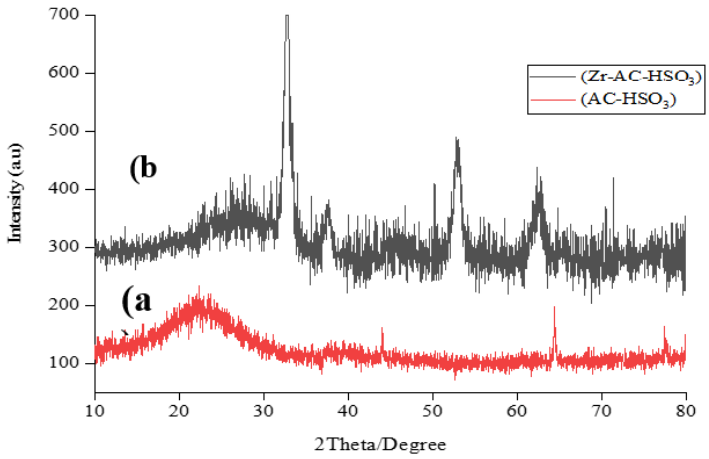

Figure 4. XRD patterns of synthesized AC-HSO_3 and 20 wt% Zr-AC-HSO_3 catalyst.

2.2.5. SEM Analysis

The SEM images of the synthesized AC-HSO_3 and 20 wt% Zr-AC-HSO_3 catalyst are compared in Figure 5a,b. The AC-HSO_3 exhibited the cluster and agglomerate shapes of the sulphonated row of activated carbon generated from the palm kernel shell material. On the contrary, the homogeneity of particles was observed over 20 wt% Zr-AC-HSO_3 catalyst, which possibly corresponded to a homogeneous dispersion of ZrO_2 loaded onto the AC-HSO_3 surface.

2.3. Optimization of Esterification Conditions

2.3.1. Effect of the Methanol:PFAD Molar Ratio

The effect of methanol (MeOH) on the FFA conversion on the esterification reaction was carried out to by altering the molar ratio of MeOH:PFAD from 5:1 to 25:1, while the other parameters of the reaction process remained constant. These parameters were catalyst concentration of 4 wt%, 75 °C operating temperature, and 4 h operating time. It was observed that the FFA conversion increased by raising the MeOH:PFAD molar ratio. The conversion of FFA increased from 70.9% to 80.8% as the molar ratio of MeOH:PFAD increased from 5:1 to 10:1. The highest FFA conversion was 85.4% at a 15:1 MeOH:PFAD molar ratio (Figure 6a). However, there was a slight decrease in the FFA conversion to

84.5% and 81.8% as the MeOH:PFAD molar ratio increased to 20:1 and 25:1, respectively. The result was in accordance with the previously reported data [22,27].

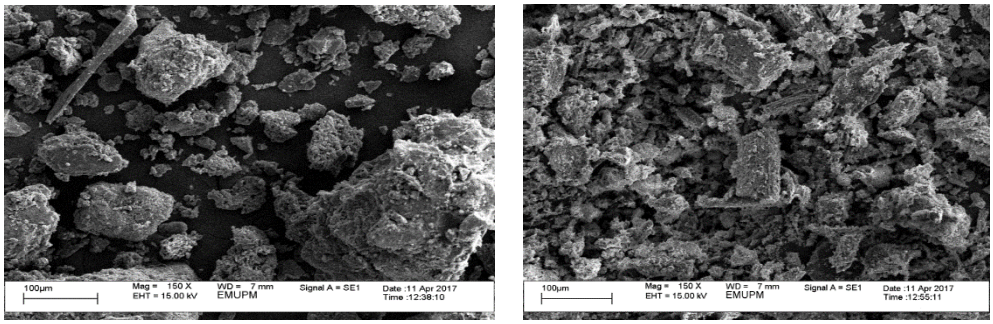

(a) **(b)**

Figure 5. SEM images of (**a**) AC-HSO_3 and (**b**) 20 wt% Zr-AC-HSO_3 catalysts.

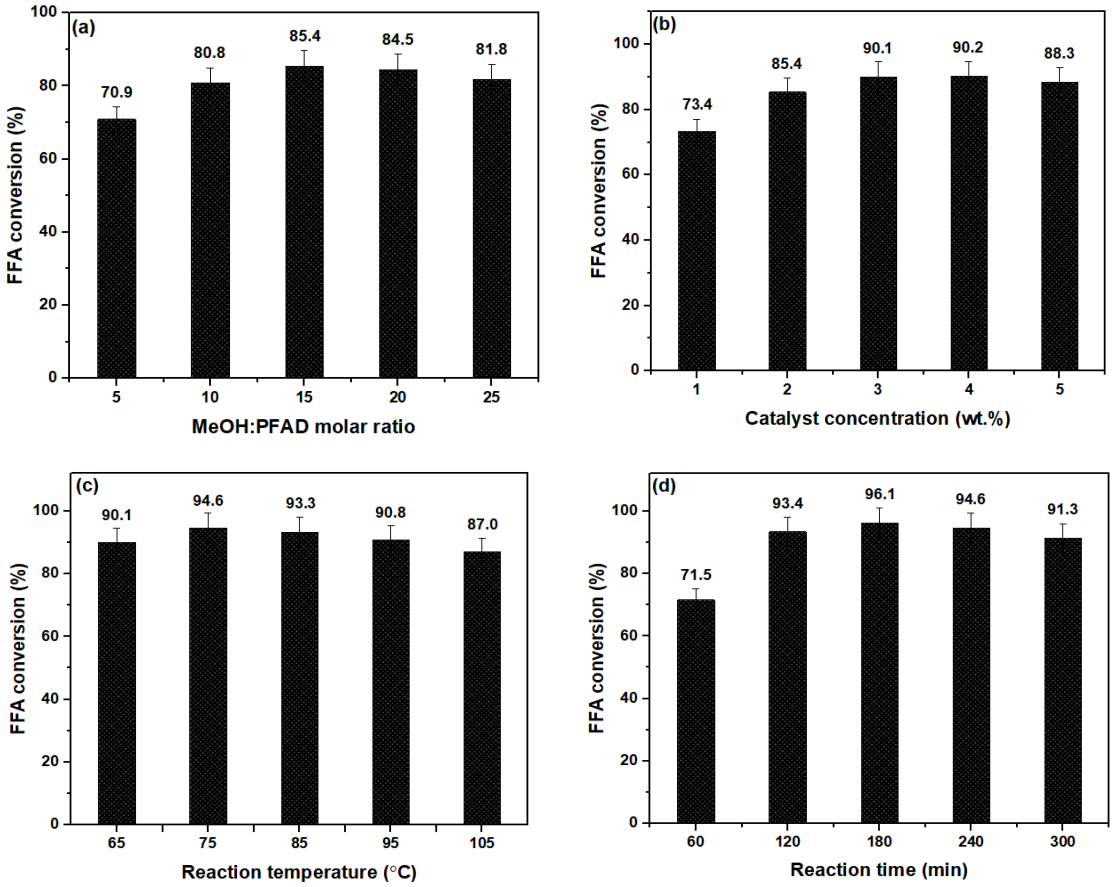

Figure 6. (**a**) Influence of MeOH:PFAD molar ratio on the FFA conversion at 4 wt% catalyst concentration, 75 °C reaction temperature and 4 h reaction time. (**b**) Influence of catalyst loading on the FFA conversion at 15:1 MeOH:PFAD molar ratio, 75 °C reaction temperature and 4 h reaction time. (**c**) Influence of reaction temperature on the FFA conversion at 15:1 MeOH:PFAD molar ratio, 3 wt% catalyst amount, and 4 h reaction time. (**d**) Influence of the time on the FFA conversion at 15:1 MeOH:PFAD molar ratio, 3 wt% catalyst amount, and 75 °C reaction temperature.

2.3.2. Effect of the Catalyst Concentration

Figure 6b depicts the effects of catalyst concentration (1 wt% to 5 wt%) on the conversion of FFA in the esterification at 15:1 MeOH:PFAD molar ratio and 75 °C for 4 h. The esterification operation is also known as a reversible reaction. The reversible esterification cannot be completed if the dosage of

the catalyst is insufficient, which commonly occurs. Therefore, the concentration of the catalyst should be sufficient to catalyze both reactions because an excessive or insufficient catalyst loading may alter the maximum FFA conversion. Characteristically, an excess amount of the catalyst raises the number of active sites, which, in turn, raises the rate of conversion with a shorter reaction time. There was a considerable increase in the FFA conversion as the catalyst loading was increased from 1 wt% to 3 wt%, recording the maximum conversion of 90.1%. However, by applying a higher amount of the 20 wt% Zr-AC-HSO_3 catalyst, the FFA conversion of the final product appeared to level off and then, slightly decrease. Therefore, the optimum concentration of the 20 wt% Zr-AC-HSO_3 catalyst was determined to be 3 wt%, by which 90.1% of FFA conversion was achieved.

2.3.3. Effect of the Operating Temperature

The influence of the operating temperature on the catalytical activity of the synthesized 20 wt% Zr-AC-HSO_3 in the PFAD esterification was investigated as presented in Figure 6c. The result demonstrated that the FFA conversion varied from 90.1% to 94.6% as the operating temperature was changed from 65 °C to 75 °C. However, further increasing the operational temperature resulted in a lower FFA conversion. This confirmed that raising the process temperature enhanced the kinetics of catalytic reaction to a certain level. Nevertheless, excessively increasing the temperature for the reaction promoted the formation of undesirable products through the process of oligomerization, which also led to a decrease in the formation of the desired product (FAME). The results were in close accordance with articles published previously [28,29].

2.3.4. Effect of the Reaction Time

The influence of the reaction time needed for the esterification of PFAD with methanol is illustrated in Figure 6d, where 1 to 5 h of reaction time were employed at a 15: 1 MeOH:PFAD molar ratio, 3 wt% catalyst concentration, and 75 °C reaction temperature. The FFA conversion was increased with time, recording the maximum of 96.1% after 3 h. It is noted that the esterification reaction required enough time to complete the transformation of FFA to FAME. However, an insufficient reaction time may result in unstable suspensions due to the presence of un-reacted methanol. As seen in Figure 6d, prolonging the reaction time beyond the optimum period caused a slight reduction in the FFA conversion, which corresponded with a change in the reaction equilibrium to a backward direction [30].

2.4. Proposed Mechanism for Esterification Reaction

The esterification of FFA with alcohol into the corresponding alkyl ester in the presence of an acidic catalyst is a fast and efficient method of the ester production. Acid catalysts such as Brønsted- and Lewis-type acids, provide the acidic sites for efficient conversion of FFA into the esters. We proposed here that an oxoniom ion initiates protonation of the carboxylic acid group, which is prone to attack by an alcohol molecule. Figure 7 depicts the step-wise acid-catalyzed esterification reaction and production of ester as follows: (i) a proton shifts from the Brønsted acid catalyst onto the FFA molecule; (ii) an intermediate is formed by a combination of the protonated carbonyl group and alcohol followed by a proton shift from one oxygen to another; (iii) when the intermediate is converted into a protonated ester, a water molecule is produced and the catalyst receives a proton from the ester.

2.5. FAME Yield Evaluation

The FAME yield was evaluated from the esterification of PFAD with methanol under the optimized operating parameters, which were a 15:1 MeOH:PFAD molar ratio, 3 wt% catalyst concentration, 75 °C reaction temperature, and 3 h reaction time, using Equation (2). The obtained FFA conversion was 96.1% and the FAME yield was 94.3%, as shown in Figure 8.

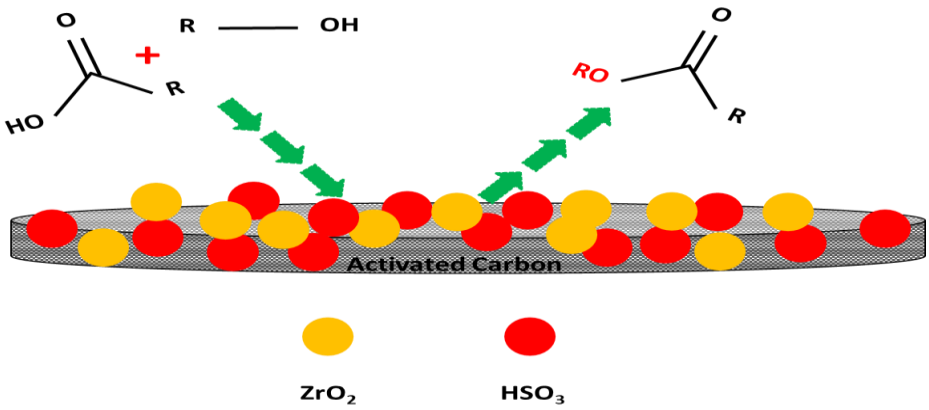

Figure 7. Proposed mechanism of the esterification reaction in the presence of the Zr-AC-HSO_3 catalyst.

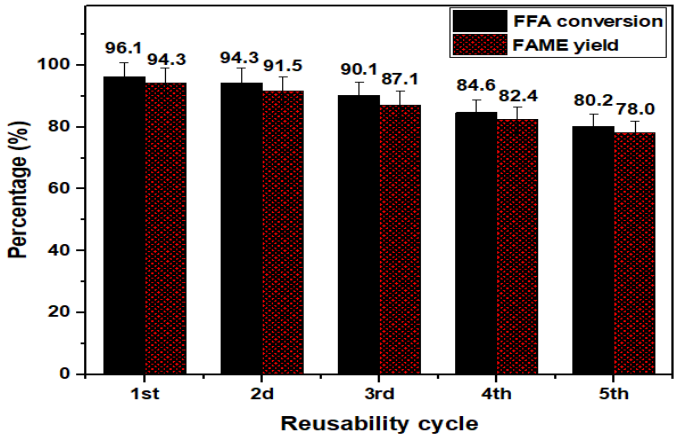

Figure 8. Reusability cycles of the synthesized 20 wt% Zr-AC-HSO_3 catalyst in the esterification of PFAD with methanol to FAME using a 15:1 MeOH:PFAD molar ratio, 3 wt% catalyst concentration, 75 °C reaction temperature and 3 h reaction time.

2.6. Catalyst Stability and Recyclability

The recyclability of the spent catalyst has been considered to be the main aspect of the reaction catalyzed via a heterogeneous route, with an aim to reduce the production cost [31]., The optimized reaction conditions; MeOH:PFAD molar ratio of 15:1, catalyst concentration of 3 wt%, reaction temperature of 75 °C and reaction time of 3 h were used in the current recycling study. In this regard, when each reaction cycle was completed, a centrifugation technique was utilized to separate the spent catalyst from the reaction mixture. After that, the spent catalyst was washed with ethanol, followed by drying in an electric oven at 120 °C for 24 h. The spent catalyst was used in all of the subsequent cycles without further regeneration of the catalytic active phase. The content of FAME was found to be 94.3%, 91.5%, 87.1%, 82%, and 78%, as illustrated in Figure 8. The spent 20 wt% Zr-AC-HSO_3 catalyst was stable for five consecutive reaction runs, and the catalytic activity decreased by only 16.3% after the fifth run. The CHNS elemental analysis indicated a decrease in the amount of sulphur from 4.80 wt% to 2.55 wt%, for the catalyst used in first and the fifth cycle. A high recyclability of the synthesized 20 wt% Zr-AC-HSO_3 catalyst might correspond to small amount of the SO_3H groups leached during the reaction because SO_3H moieties were strongly attached to the carbon surface of the synthesized catalyst.

2.7. Comparison of Zr-Based Catalysts in the Ester Production

In Table 2, a comparison of different types of Zr-based catalysts in the esterification to produce biodiesel is presented. It was observed that different Zr-based catalysts required a large methanol-to-feedstock molar ratio but in the present study, the Zr-AC-HSO_3 catalyst required a

molar ratio of 15:1 and gave a high ester yield of 96.1%. Moreover, our Zr-AC-HSO_3 catalyst gave very promising results at mild reaction conditions when compared to other studies, regarding less amount of methanol consumed and low reaction temperature required. In our present study, we used the waste material for producing the activated carbon, which makes it cheaper compared to other Zr-based catalysts.

Table 2. Comparison of Zr-based catalysts in the ester production.

Catalyst	MeOH:Feedstock Molar Ratio	Catalyst Concentration	Reaction Time	Reaction Temperature	Ester Yield	Reference
SO_4^{2-}/ZrO_2	12.7:1	2.9	93	148.5	93.5	[32]
$Mg_2Zr_5O_{12}$	18:1	2.5	150	135	97.0	[33]
ZrO_2/BLA	15:1	15	60	-	95.9	[34]
ZrO_2/SiO_2	120:1	0.1	180	120	48.6	[35]
Zr-AC-HSO_3	15:1	20	180	75	96.1	This work

2.8. Determination of Physicochemical Characteristics of Synthesized PFAD Methyl Ester

In this research, seven key FAME characteristics were determined. They were the kinematic viscosity, specific gravity, water content, flash point, cloud point, pour point, and acid value. The analysis was made three times for each experiment, and the mean ± standard deviations were utilized to report the results. These characteristics were later used in comparison with the EN14214 and the ASTMD6751 specifications as summarized in Table 3.

Table 3. Fuel characteristics of the FAME product synthesized over the 20 wt% Zr-AC-HSO_3 catalyst.

Characteristics	FAME Product	Method	ASTM D6751	EN 14214
Specific gravity (g cm^{-3})	0.83 ± 0.10	ASTM D1298	0.82–0.90	0.86–0.90
Kinematic viscosity (mm^2 s^{-1})	4.19 ± 0.07	ASTM D445	1.9–6.0	3.5–5.0
Cloud point (°C)	9 ± 0.50	ASTM D2500	−3–12	⁂ NS
Pour point (°C)	6 ± 0.30	ASTM D97	−15–12	⁂ NS
Flash point (°C)	170 ± 3.30	ASTM D93	130 min	120 min
Acid value (mg KOH g^{-1})	0.39 ± 0.07	ASTM D664	0.5 max	0.5 max
Water content (mg kg^{-1})	0.01 ± 0.01	ASTM D6304	0.03 max	0.05 max

⁂ Not specified. EN 14214 uses time and location-dependent values for cloud point and pour point.

2.8.1. Specific Gravity

The specific gravity of biodiesel production can be described as the ratio of the water to the FAME density at 15 °C, which highly depends on the set temperature and the nature of the catalyst used [36–38]. According to the EN14214 and ASTM D-1298 standards, the biodiesel density should range from 0.82–0.90 g cm^{-3} to 0.86–0.90 g cm^{-3}, respectively. Expectedly, the density of the synthesized PFADME was 0.83 g cm^{-3}, which was reasonably less than the purified PFAD's density (0.92 g cm^{-3}). Whilst the density of synthesized FAME was lower than that of the current diesel fuel, it still satisfied both sets of standards, i.e., the EN 14214 and the ASTM D1298.

2.8.2. Kinematic Viscosity

Another important fuel characteristic is kinematic viscosity (KV). The high viscosity of current petroleum is the main barrier to the proper atomization of petroleum while it is running into the chamber. The high viscosity of the current fuel is attributed to its long carbon chains, as well as its heavy molecular weight. One approach to reducing KV is to increase the operating temperature to break the carbon chains, which results in carbon chains that are shorter in length [39,40]. In this regard, an appropriate catalyst is required to keep it highly stable at higher operating temperatures. The KV value of the FAME ranged from 3.5 to 5.0 mm^2s^{-1} and 1.9 to 6.0 mm^2s^{-1} by following the EN14214

and ASTM D6751, respectively. However, the value of the KV for the synthesized PFADME was 4.19 mm^2s^{-1}, but it remained in the range of the specified standards.

2.8.3. Cold Flow Characteristics

The pour point (PP) and cloud point (CP) are two main low temperature features of fuel. The PP is the temperature at which a fluid begins to flow, and the CP is the temperature at which fuel begins to solidify as it cools down. To avoid freezing the oil in a cold environment, the PP and CP values should be satisfactorily low. The CP of the synthesized ester was found to be 9 °C, whilst the PP value was 6 °C, as shown in Table 3. The average CP and PP values obtained, can ease the flow of the fuel as it passes through the plug filtering.

2.8.4. Flash Point

The flash point (FP) is described as temperature at which oil tends to vaporize to produce an combustible mixture in the presence of oxygen. Knowing that the FP of the fuel is highly important for the safe transportation and storage of fuel, the current synthesized biodiesels possess low FP values in comparison with conventional petroleum. For the present research, the FP value was observed to be 170 °C. This was acceptably in accordance with the limits fixed in both the EN 14214 and ASTM D93 standards.

2.8.5. Acid Value

Another key feature of petroleum is the acid value (AV) because the existence of FFA in the fuel could result in erosion of the metallic items in the engine. It is usually measured by the titration method, which shows the mass of KOH that neutralizes 1 g of the oil's acidic components. The AV of the synthesized ester was 0.39 mg KOH/g, which met the EN 14214 and ASTM D664 standard limits.

2.8.6. Water Content

When water is present in the fuel, it may cause the tank to corrode, suspensions to form, bacterial improvement, and hydrolytic oxidation to occur [41]. However, synthesized fuel is dried to eliminate the existence of moisture; although it may become moisturized during the process of transportation or storage. In this study, the value of the water content of the synthesized PFADME was 0.01%, which was lower than the specified values of the ASTM D6304 and EN14214 specifications.

3. Materials and Methods

3.1. Materials

The palm kennel shell and PFAD were procured from Jomalina R&D Sime Darby Sdn. Bhd. Malaysia. Zirconium hydroxide $Zr(OH)_4$, potassium hydroxide (KOH), concentrated chlorosulphonic acid ($HClSO_4$), methanol (CH_3OH), and ethanol (CH_3CH_2OH) were sourced by Merck Chemicals, Malaysia. Furthermore, sodium sulphate (Na_2SO_4) was provided by Sigma-Aldrich. The standard methyl esters used for the gas chromatography (GC) analysis, such as methyl heptadecanoate, methyl myristate, methyl palmitate, methyl linoleate, and methyl oleate, were provided by Fluka, USA. All of these reagents and chemicals were provided, commercially, in analytical grade and were utilized as provided with no other process of purification.

3.2. FAME Analysis

FAME was produced by the esterification of PFAD using a batch system. As the reaction process was completed, the obtained reaction mixture was analyzed to measure the FFA conversion and FAME yield. The FFA conversion was assessed by calculating the differentiation between the acid values of final product and feedstock based on the standard technique for AOCS 5a-40 using Equation (1) [42]

$$\textbf{FFA}\ (\%) = \frac{\mathbf{AV_{feedstock} - AV_{product}}}{\mathbf{AV_{feedstock}}} \times \mathbf{100} \quad (1)$$

Concurrently, the FAME yield analysis was carried out using a gas chromatography with flame ionization detector (GC-FID). Separation of organic compounds in the FAME product was achieved by using a highly-polar capillary column BPX-70 that had an internal diameter of 0.25 mm and a length of 30 m. During the process of analysis, 500 ppm of each of the FAME standards was prepared as reference standards using n-hexane as a solvent. At the same time, methyl heptadecanoate was prepared along with the sample product and utilized as the internal standard. About 1 µL of the sample, which had been prepared, was applied to the injection port of GC. The detector temperature was set at 270 °C, while the injector port was fixed at 230 °C. In addition, the column oven programmed to increase the temperature from 100 °C, at a heating rate of 10 °C/min, to 250 °C. Equation (2) was used for the calculation of the FAME yield [43].

$$\textbf{FAME Yield}\ (\%) = \frac{\sum \mathbf{A} - \mathbf{A_{EI}}}{\mathbf{A_{EI}}} \times \frac{\mathbf{C_{EI}} \times \mathbf{V_{EI}}}{\mathbf{M}} \times \mathbf{100} \quad (2)$$

where, the total area of C14-C18 FAME peaks was represented as ∑A, the peak area of the internal standard was represented as AEI, the amount of the internal standard (mg/mL) was represented as CEI, the volume of the internal standard (mL) was represented as VEI, and the mass of the sample (mg) was represented as M.

3.3. Catalyst Preparation

The simple wet impregnation technique was introduced to prepare the catalyst as shown by the schematic design in Figure 9. In order to remove any dirt from the palm kennel shell, it was washed thoroughly using ethanol and then oven-dried at 120 °C. Subsequently, using a miller, the dried shell of the palm kennel was crushed into powder form before calcination at 600 °C for 4 h under the flow of nitrogen gas (N_2). The activated carbon (AC) was impregnated with the required stoichiometric amount of $Zr(OH)_4$, making Zr-AC, and was stirred vigorously on a magnetic stirrer for 5 h. The resultant slurry was oven dried for 24 h at 120 °C. This dried sample was post-calcined for 3 h at 650 °C. Later, concentrated chlorosulphonic acid was used to sulphonate the catalyst for 2 h at 120 °C; after which, the sulphonated Zr-AC-HSO_3 catalyst was washed with distilled water until the water had a pH value of 7. The washed catalyst underwent further drying in an oven at 65 °C for 12 h. The resultant material was annealed at a temperature of 400 °C for 3 h. The same procedure was carried out to prepare the 10 wt%, 15 wt%, 20 wt%, and 25 wt% ZrO_2-doped sulphonated catalyst samples, respectively.

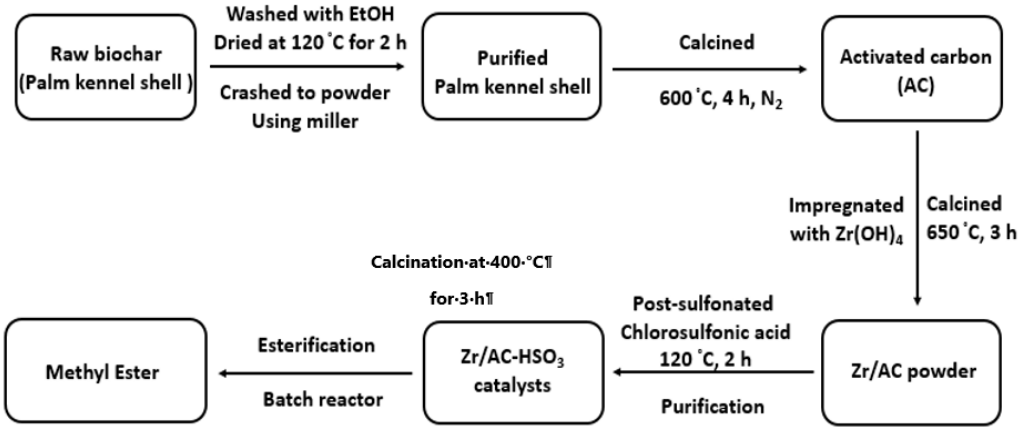

Figure 9. Schematic design of preparation of ZrO_2-doped sulfonated biochar catalysts, using the wet impregnation method, for FAME preparation.

3.4. Catalytic Activity

The catalytic performance of the catalyst was then studied by way of the esterification of PFAD. Prior to esterification, any moisture and impurities of any other kind were eliminated from the feedstock to gain a high yield. In this regard, PFAD was heated for 30 min at 110 °C, and then it was filtered by using sodium sulphate (Na_2SO_4) as the agent for drying and removing any moisture that remained.

Typically, the esterification reaction took place using 10 g of the PFAD, a certain amount of the Zr-AC-HSO_3 carbon-based catalyst, and methanol. These items were mixed in a 100 mL round-bottom flask possessing a cool water condenser. A predefined temperature was set to heat the mixture whilst it was stirred vigorously over a magnetic stirrer hot plate. When each reaction had completed, 6000 rpm was used to centrifuge the suspension for 15 min so that the phases could be separated; then, the mixture phase was heated so that the methanol could be evaporated. The product was further analyzed to determine the FFA conversion rate and the FAME yield using specified equations. All of the optimization and reproducibility studies were performed in triplicate sets and the results are presented in Figures 6 and 7 as the mean ± standard deviation for the statistical analysis.

3.5. Catalyst Characterization

The determination of the synthesized Zr-AC-HSO_3 catalyst structural analysis was made using the XRD technique, by employing the Shimadzu 6700 model. The analysis was run by Cu–K radiation in the range of 5–70° 2θ angle at a 4 °C/min scanning rate. The Brunauer–Emmett–Teller (BET) model evaluated textural feathers of the synthesized Zr-AC-HSO_3 catalyst, using Thermo Finningan Italia S.P.A. The Barrett–Joyner–Halenda (BJH) determined the pore distribution diameters and adsorption–desorption isotherm methods were used to measure the specific surface areas of the catalyst samples. assessed by and Primarily, the catalyst samples were degassed and dehydrated at 150 °C for 2 h in the presence of hydrogen flow. Later. Tube containing catalysts samples were soaked into N_2 (−196 °C). The amount of N_2 adsorption was computed to the relative pressure. The temperature programmed desorption of NH_3 was introduced to evaluate the acidity of the synthesized Zr-AC-HSO_3 catalyst. The analysis was carried out using an 1100 series of the Thermo Finnigan TPD/R/O, which possessed a detector for thermal conductivity (TCD). The samples were pre-heated at 250 °C for 30 min under a flow of N_2, before being subjected to analysis, in order to obtain a clean surface and to eliminate any undesired contaminants. The desorption of the NH_3 was achieved under the gas flow of NH_3 for a period of 60 min. Thereafter, the sample was pre-treated further by removing any excess NH_3 under a helium gas flow. The samples were preheated to 700 °C at a heating rate increment of 10 °C/min with a 30 mL/min flow rate under the flow of helium for 30 min. Finally, the content amount of the desorbed NH_3 was detected and recorded using a TCD. The determination of the chemical functional groups present on the surface of the synthesized Zr-AC-HSO_3 catalyst was made using the analysis done by using Fourier transform infrared (FT-IR) spectroscopy at a range of wavelengths from 400 to 4000 cm^{-1}. The sample was initially filled in the sample cup holder and inserted into the instrument for scanning. The absorption frequency spectra of the sample were recorded and plotted as the transmittance (%) against the wave number (cm^{-1}). In this study, the FT-IR spectroscopy (SHIMADZU Model) was employed to identify the various functional groups present in the prepared samples. The morphologies of the samples of the catalyst were determined by a Nova Nanosem 30 series microscope (FEI Company, Oregon, USA) using 5 kV. The samples of the catalyst were layered with gold by employing a sputter coating method before they were analyzed.

4. Conclusions

The wet impregnation technique was used to prepare a Zirconium-doped sulphonated activated carbon-based (Zr-AC-HSO_3) catalyst and was then successfully used for FAME production, using a PFAD feedstock. The results revealed the importance of varying the loading of the zirconium into activated carbon-based catalysts on the catalytic activity. A remarkable FAME yield of 94.3% and

FFA conversion of 96.1% were obtained using the optimised reaction conditions, consisting of a 15:1 MeOH:PFAD molar ratio, 3 wt% catalyst loading, 75 °C reaction temperature, and 3 h reaction time. The stability of the catalyst was determined, and it was found that 20 wt% Zr-AC-HSO_3 had a high potential to stay active even after five consecutive cycles. The synthesized 20 wt% Zr-AC-HSO_3 catalyst also exhibited a great potential for the FAME production with excellent fuel properties in line with the specified limits in both the ASTM D6751 and the EN14214 standards.

Author Contributions: Conceptualization, U.R., S.S.; data curation, S.S., J.A.; writing—original draft preparation, U.R., S.S.; J.A.; writing—review and editing, T.S.Y.C.; I.A.N., C.N.

Funding: The authors acknowledge their gratitude to King Saud University (Riyadh, Saudi Arabia) for the funding of this research through Researchers Supporting Project number (RSP-2019/80). In addition, the authors want to extend their profound gratitude for the financial support from the Universiti Putra Malaysia under project GP-IPB/2016/9490400.

Acknowledgments: Authors are thankful to Balkis Hazmi and Nasar Mansir for their technical support during this project.

Conflicts of Interest: There has been no conflict of interest declared by the authors.

References

1. Malins, K. The potential of K_3PO_4, K_2CO_3, Na_3PO_4 and Na_2CO_3 as reusable alkaline catalysts for practical application in biodiesel production. *Fuel. Proc. Technol.* **2018**, *179*, 302–312. [CrossRef]
2. Soltani, S.; Rashid, U.; Al-Resayes, S.I.; Nehdi, I.A. Recent progress in synthesis and surface functionalization of mesoporous acidic heterogeneous catalysts for esterification of free fatty acid feedstocks: A review. *Energy Convers. Manag.* **2017**, *141*, 183–205. [CrossRef]
3. Baskar, G.; Aiswarya, R. Trends in catalytic production of biodiesel from various feedstocks. *Renew. Sustain. Energy Rev.* **2016**, *57*, 496–504. [CrossRef]
4. Rashid, U.; Rehman, H.A.; Hussain, I.; Ibrahim, M.; Haider, M.S. Muskmelon (*Cucumis melo*) seed oil: A potential non-food oil source for biodiesel production. *Energy* **2011**, *36*, 5632–5639. [CrossRef]
5. Zhao, C.; Yang, L.; Xing, S.; Luo, W.; Wang, Z.; Lv, P. Biodiesel production by a highly effective renewable catalyst from pyrolytic rice husk. *J. Clean. Prod.* **2018**, *199*, 772–780. [CrossRef]
6. Lu, Y.; Zhang, Z.; Xu, Y.; Liu, Q.; Qian, G. CaFeAl mixed oxide derived heterogeneous catalysts for transesterification of soybean oil to biodiesel. *Bioresour. Technol.* **2015**, *190*, 438–441. [CrossRef]
7. Kazemian, H.; Turowec, B.; Siddiquee, M.N.; Rohani, S. Biodiesel production using cesium modified mesoporous ordered silica as heterogeneous base catalyst. *Fuel* **2013**, *103*, 719–724. [CrossRef]
8. Dehkordi, A.M.; Ghasemi, M. Transesterification of waste cooking oil to biodiesel using Ca and Zr mixed oxides as heterogeneous base catalysts. *Fuel Process. Technol.* **2012**, *97*, 45–51. [CrossRef]
9. Ouedraogo, I.W.K.; Mouras, S.; Changotade, O.A.; Blin, J. Development of new solid acid catalyst for biodiesle production using local vegetable resources, adapted to the contexts of the West African countries. *Waste Biomass Valor.* **2018**, *9*, 1893–1901. [CrossRef]
10. Martinez, A.; Mijangos, G.E.; Romeoro-Ibarra, I.C.; Hernandez-Altamirano, R.; Mena-Cervantes, V.Y.; Gutierrez, S. A novel green one-pot synthesis of biodiesel from *Ricinus communis* seeds by basic heterogeneous catalysis. *J. Clean. Prod.* **2018**, *196*, 340–349. [CrossRef]
11. Galadima, A.; Muraza, O. Biodiesel production from algae by using heterogeneous catalysts: A critical review. *Energy* **2014**, *78*, 72–83. [CrossRef]
12. Malins, K.; Kampars, V.; Brinks, J.; Neibolte, I.; Murnieks, R. Synthesis of activated carbon based heterogenous acid catalyst for biodiesel preparation. *Appl. Catal. B Environ.* **2015**, *176–177*, 553–558. [CrossRef]
13. Yujaroen, D.; Goto, M.; Sasaki, M.; Shotipruk, A. Esterification of palm fatty acid distillate (PFAD) in supercritical methanol: Effect of hydrolysis on reaction reactivity. *Fuel* **2009**, *88*, 2011–2016. [CrossRef]
14. Cho, H.J.; Kim, S.H.; Hong, S.W.; Yeo, Y.-K. A single step non-catalytic esterification of palm fatty acid distillate (PFAD) for biodiesel production. *Fuel* **2012**, *93*, 373–380. [CrossRef]
15. Nakajima, K.; Hara, M. Amorphous carbon with SO_3H groups as a solid Brønsted acid catalyst. *Am. Chem. Soc. Catal.* **2012**, *2*, 1296–1304. [CrossRef]

16. Wang, A.; Li, H.; Pan, H.; Zhang, H.; Xu, F.; Yu, Z.; Yang, S. Efficient and green production of biodiesel catalyzed by recyclable biomass-derived magnetic acids. *Fuel Process. Technol.* **2018**, *181*, 259–267. [CrossRef]
17. Konwar, L.J.; Boro, J.; Deka, D. Review on latest developments in biodiesel production using carbon-based catalysts. *Renew. Sustain. Energy Rev.* **2014**, *29*, 546–554. [CrossRef]
18. Kastner, J.R.; Miller, J.; Geller, D.P.; Locklin, J.; Keith, L.H.; Johnson, T. Catalytic esterification of fatty acids using solid acid catalysts generated from biochar and activated carbon. *Catal. Today* **2012**, *190*, 122–132. [CrossRef]
19. Lou, W.-Y.; Zong, M.-H.; Duan, Z.-Q. Efficient production of biodiesel from high free fatty acid-containing waste oils using various carbohydrate-derived solid acid catalysts. *Bioresour. Technol.* **2008**, *99*, 8752–8858. [CrossRef]
20. Chin, L.H.; Abdullah, A.Z.; Hameed, B.H. Sugar cane bagasse as solid catalyst for synthesis of methyl esters from palm fatty acid distillate. *Chem. Eng. J.* **2012**, *183*, 104–107. [CrossRef]
21. Lokman, I.M.; Rashid, U.; Taufiq-Yap, Y.H. Production of biodiesel from palm fatty acid distillate using sulfonated-glucose solid acid catalyst: Characterization and optimization. *Chin. J. Chem. Eng.* **2015**, *23*, 1857–1864. [CrossRef]
22. Soltani, S.; Rashid, U.; Al-Resayes, S.I.; Nehdi, I.A. Sulfonated mesoporous ZnO catalyst for methyl esters production. *J. Clean. Prod.* **2017**, *144*, 482–491. [CrossRef]
23. Dawodu, F.A.; Ayodele, O.; Xin, J.; Zhang, S.; Yan, D. Effective conversion of non-edible oil with free fatty acid into biodiesel by sulphonated carbon catalyst. *Appl. Energy* **2014**, *114*, 819–826. [CrossRef]
24. Soltani, S.; Rashid, U.; Nehdi, I.A.; Al-Resayes, S.I.; Al-Muhtaseb, A.H. Sulfonated mesoporous zinc aluminate catalyst for biodiesel production from high free fatty acid feedstock using microwave heating system. *J. Taiwan Instit. Chem. Eng.* **2017**, *70*, 219–228. [CrossRef]
25. Liu, X.-Y.; Huang, M.; Ma, H.-L.; Zhang, Z.-Q.; Gao, J.-M.; Zhu, Y.-L.; Han, X.-J.; Guo, X.-Y. Preparation of a carbon-based solid acid catalyst by sulfonating activated carbon in a chemical reduction process. *Molecules* **2010**, *15*, 7188–7196. [CrossRef]
26. Duan, G.; Zhang, C.; Li, A.; Yang, X.; Lu, L.; Wang, X. Preparation and characterization of mesoporous zirconia made by using a poly (methyl methacrylate) template. *Nanoscale Res. Lett.* **2008**, *3*, 118–122. [CrossRef]
27. Amani, H.; Ahmad, Z.; Hameed, B.H. Highly active alumina-supported Cs–Zr mixed oxide catalysts for low-temperature transesterification of waste cooking oil. *Appl. Catal. A Gen.* **2014**, *487*, 16–25. [CrossRef]
28. Soltani, S.; Rashid, U.; Yunus, R.; Taufiq-Yap, Y.H.; Al-Resayes, S.I. Post-functionalization of polymeric mesoporous C@Zn core-shell spheres used for methyl ester production. *Renew. Energy* **2016**, *99*, 1235–1243. [CrossRef]
29. Amani, H.; Ahmad, Z.; Asif, M.; Hameed, B.H. Transesterification of waste cooking palm oil by MnZr with supported alumina as a potential heterogeneous catalyst. *J. Ind. Eng. Chem.* **2014**, *20*, 4437–4442. [CrossRef]
30. Sirisomboonchai, S.; Abuduwayiti, M.; Guan, G.; Samart, C.; Abliz, S.; Hao, X. Biodiesel production from waste cooking oil using calcined scallop shell as catalyst. *Energy Convers. Manag.* **2015**, *95*, 242–247. [CrossRef]
31. Xie, W.; Hu, L.; Yang, X. Basic ionic liquid supported on mesoporous SBA-15 silica as an efficient heterogeneous catalyst for biodiesel production. *Ind. Eng. Chem. Res.* **2015**, *54*, 1505–1512. [CrossRef]
32. Vahid, B.R.; Saghatoleslami, N.; Nayebzadeh, H.; Toghiani, J. Effect of alumina loading on the properties and activity of SO_4^{2-}/ZrO_2 for biodiesel production: Process optimization via response surface methodology. *J. Taiwan Inst. Chem. Eng.* **2018**, *83*, 115–123. [CrossRef]
33. Singh, V.; Belova, L.; Singh, B.; Sharma, Y.C. Biodiesel production using a novel heterogeneous catalyst, magnesium zirconate ($Mg_2Zr_5O_{12}$): Process optimization through response surface methodology (RSM). *Energy Conver. Manag.* **2018**, *174*, 198–207. [CrossRef]
34. Fatimah, I.; Rubiyanto, D.; Taushiyah, A.; Najah, F.B.; Azmi, U.; Sim, Y.-L. Use of ZrO_2 supported on bamboo leaf ash as a heterogeneous catalyst in microwave-assisted biodiesel conversion. *Sustain. Chem. Pharm.* **2019**, *12*, 100129. [CrossRef]
35. Ibrahim, M.M.; Mahmoud, H.R.; El-Molla, S.A. Influence of support on physicochemical properties of ZrO_2 based solid acid heterogeneous catalysts for biodiesel production. *Catal. Commun.* **2019**, *122*, 10–15. [CrossRef]

36. Dinkov, R.; Hristov, G.; Stratiev, D.; Aldayri, V.B. Effect of commercially available antioxidants over biodiesel/diesel blends stability. *Fuel* **2009**, *88*, 732–737. [CrossRef]
37. Ganduglia-Pirovano, M.V.; Popa, C.; Sauer, J.; Abbott, H.; Uhl, A.; Baron, M. Role of ceria in oxidative dehydrogenation on supported vanadia catalysts. *J. Am. Chem. Soc.* **2010**, *132*, 2345–2349. [CrossRef]
38. Du, J.; Xu, H.; Shen, J.; Huang, J.; Shen, W.; Zhao, D. Catalytic dehydrogenation and cracking of industrial dipentene over M/SBA-15 (M=Al, Zn) catalysts. *Appl. Catal. A Gen.* **2005**, *296*, 186–193. [CrossRef]
39. Lin, C.-Y.; Chiu, C.-C. Burning characteristics of palm-oil biodiesel under long-term storage conditions. *Energy Convers. Manag.* **2010**, *51*, 1464–1467. [CrossRef]
40. Lin, C.-Y.; Cheng, H.-H. Application of mesoporous catalysts over palm-oil biodiesel for adjusting fuel properties. *Energy Convers. Manag.* **2012**, *53*, 128–134. [CrossRef]
41. Knothe, G. Analyzing biodiesel: Standards and other methods. *J. Am. Oil Chem. Soc.* **2006**, *83*, 823–833. [CrossRef]
42. Rao, B.V.S.K.; Mouli, K.C.; Rambabu, N.; Dalai, A.K.; Prasad, R.B.N. Carbon-based solid acid catalyst from de-oiled canola meal for biodiesel production. *Catal. Commun.* **2011**, *14*, 20–26. [CrossRef]
43. Cho, H.J.; Kim, J.-K.; Hong, S.W.; Yeo, Y.-K. Development of a novel process for biodiesel production from palm fatty acid distillate (PFAD). *Fuel Process. Technol.* **2012**, *104*, 271–280. [CrossRef]